Marshall University
Marshall Digital Scholar

Chemistry Faculty Research | Chemistry

1996

Substitution Reactions of (C5Ph5)Cr(CO)3: Structural, Electrochemical, and Spectroscopic Characterization of (C5Ph5)Cr(CO)2L, L = PMe3, PMe2Ph, P(OMe)3

D. John Hammack

Mills M. Dillard

Michael Castellani
Marshall University, castella@marshall.edu

Arnold L. Rheingold

Anne L. Rieger

See next page for additional authors

Recommended Citation

Hammack, D. J.; Dillard, M. M.; Castellani, M. P.; Rheingold, A. L.; Rieger, A. L.; Rieger, P. H., Substitution Reactions of (C5Ph5)Cr (CO)3: Structural, Electrochemical, and Spectroscopic Characterization of (C5Ph5)Cr(CO)2L (L= PMe3, PMe2Ph, P (OMe)3). Organometallics 1996, 15 (22), 4791-4797.

Authors
D. John Hammack, Mills M. Dillard, Michael Castellani, Arnold L. Rheingold, Anne L. Rieger, and Philip H. Rieger

Substitution Reactions of $(C_5Ph_5)Cr(CO)_3$: Structural, Electrochemical, and Spectroscopic Characterization of $(C_5Ph_5)Cr(CO)_2L$, L = PMe_3, PMe_2Ph, $P(OMe)_3$

D. John Hammack,[1a] Mills M. Dillard,[1a] Michael P. Castellani,*,[1a] Arnold L. Rheingold,*,[1b] Anne L. Rieger,[1c] and Philip H. Rieger*,[1c]

Departments of Chemistry, Marshall University, Huntington, West Virginia 25755, University of Delaware, Newark, Delaware, 19716, and Brown University, Providence, Rhode Island 02912

Abstract

The radical complex, $(C_5Ph_5)Cr(CO)_3$, reacts with small, neutral, monodentate Lewis bases (PMe_3, PMe_2Ph, and $P(OMe)_3$) in THF at -78 ºC (PMe_2Ph reacts at ambient temperature) to yield the monomeric substitution products, $(C_5Ph_5)Cr(CO)_2L$•THF as thermally stable solids. Electrochemical and spectroscopic data are provided. An X-ray crystal structure of the hemisolvate $(C_5Ph_5)Cr(CO)_2PMe_3$•0.5THF was obtained. Frozen solution ESR spectra of $(C_5Ph_5)Cr(CO)_2L$ in toluene are comparable to those of other low-spin d^5 “piano-stool” complexes. Rotation of the $Cr(CO)_2L$ moiety relative to the C_5Ph_5 ring is rapid on the ESR time scale in low-temperature liquid solutions and leads to axial powder-like spectra. Analysis of this effect leads to significant insights into the electronic structure.

Introduction

Over the past two decades, the study of paramagnetic organometallic complexes has greatly expanded.[2] These complexes are generally highly reactive and many have been postulated as reaction intermediates. In particular, the $(C_5R_5)Cr(CO)_3$ (R = H, Me, Ph) family of complexes recently has received much attention. The R = H and Me complexes both exist in equilibria between 17e monomers and 18e dimers in solution and as dimers in the solid state,[3] while for R = Ph the complex exists solely as a 17e monomer both in solution and the solid state.[4]

Seventeen electron complexes containing CO ligands frequently undergo substitution reactions under mild conditions.[5,6] The reactions tend to proceed via associative mechanisms[7] because of incompletely filled sets of bonding molecular orbitals.[8] Baird and coworkers have studied extensively the substitution reactions of $(C_5R_5)Cr(CO)_3$ (R = H,[9] Me[10,9e]) with phosphines. Where R = H (Cp) isolation of a product complex requires larger phosphines, while for R = Me (Cp*) only smaller phosphines replace CO in the starting complex.

The very large size of the C_5Ph_5 ligand should significantly restrict the size of substituents that can substitute CO in $(C_5Ph_5)Cr(CO)_3$, **1**. Three small, monodentate Lewis bases, PMe_3, PMe_2Ph, and $P(OMe)_3$, react with **1** to yield isolable products, $(C_5Ph_5)Cr(CO)_2L$. These compounds have been spectroscopically and electrochemically characterized.

There have been many ESR studies of low-spin d^5 "piano-stool" complexes such as $(C_5R_5)Cr(CO)_{3-x}L_x$ (R = H, Me), $[(Arene)Cr(CO)_{3-x}L_x]^+$, and Mn(II) analogs.[11] As we will show, the ESR spectra of $(C_5Ph_5)Cr(CO)_2L$ fit comfortably into the general scheme for these complexes and are thus rather unremarkable. However, the unique steric bulk of the C_5Ph_5 ligand leads to selective averaging of anisotropies in the ESR spectra of low-temperature liquid solutions, and parameters obtained from such spectra provide insights into the electronic structure which were unavailable in previous studies.

Experimental Section

General Data. All reactions of air- and moisture-sensitive materials were performed under a nitrogen atmosphere employing standard Schlenk techniques unless otherwise stated. Solids were manipulated under nitrogen or argon in a Vacuum Atmospheres glovebox equipped with a HE-493 dri-train. Solvents (Fisher) were distilled from the appropriate drying agent under argon: toluene, hexane (sodium/benzophenone), benzene, tetrahydrofuran (THF) (potassium/benzophenone), and dichloromethane (CaH_2). $(C_5Ph_5)Cr(CO)_3 \cdot C_6H_6$ was prepared according to a literature procedure.[4] NMR solvents were vacuum distilled from CaH_2 and placed under an argon atmosphere. PPh_3 (PCR) was recrystallized from 95% ethanol. PMe_3, PMe_2Ph, $P(OMe)_3$, $P(OPh)_3$ (Strem), $CDCl_3$, CD_2Cl_2 (Aldrich), 2,2'-bipyridine (Matheson), diphenylacetylene (Eastman), and all other solvents (Fisher) were used without further purification. Elemental analyses were performed by Schwartzkopf Microanalytical Laboratory, Woodside, N.Y and Mickroanalytisches Labor Pascher, Remagen, Germany. ^{1}H (200.06 MHz) and ^{31}P (80.962 MHz) NMR spectra were obtained on a Varian XL-200 NMR spectrometer equipped with a Motorola data system upgrade.

Electrochemistry. Electrochemical data were obtained on a EG&G PAR VersaStat Model 250-1 Electrochemical Analysis system. The apparatus was maintained on a bench top under constant nitrogen purge. Freshly distilled CH_2Cl_2 was employed as the solvent, with a supporting electrolyte of 0.1 M $^{n}Bu_4NPF_6$ (recrystallized from 95% ethanol). Solutions were *ca*. 3 mM in complex.[12] Decamethylferrocene was added as an internal reference. Potentials are referred to the ferrocene/ferrocenium couple. All data were obtained with a Pt disk working electrode (r = 1.6 mm) and either a Ag/AgCl reference electrode or a AgCl coated Ag wire reference electrode.

ESR Spectroscopy. Electron spin resonance spectra were obtained using a Bruker ER-220D X-band spectrometer equipped with a Bruker variable temperature accessory, a Systron-Donner microwave frequency counter and a Bruker gaussmeter. Samples for ESR study were prepared in an argon-filled glove box by shaking the compound with degassed toluene to obtain a saturated solution; the solution was syringed into an ESR tube which was sealed with Parafilm before removal from the glove box. One series of spectra was obtained with 5 mg of the

$P(OMe)_3$ complex in 3 mL of 1:1 1,2-$C_2H_4Cl_2$/CH_2Cl_2 (dce/dcm); the solution was prepared in a glove box as before.

X-ray Structural Determination. Crystallographic data are summarized in Table 1. A specimen mounted on a glass fiber was found photographically to possess only triclinic symmetry. The centrosymmetric space group was initially assumed and later supported by the reasonable results of refinement. Variation in azimuthal scans were less than 10% and corrections for absorption were ignored. The structure was solved by direct methods. The asymmetric unit is composed of two cyrstallographically independent but chemically very similar molecules of the Cr complex and one molecule of THF. All non-hydrogen atoms were refined with anisotropic displacement parameters. Selected bond distances and angles are collected in Tables 2 and 3, respectively. Phenyl dihedral angles are presented in Table 4. All computations used SHELXTL 4.2 programs (G. Sheldrick, Siemens XRD, Madison, WI).

Low Temperature IR Spectroscopy. In a glovebag, a dilute solution of **1** in THF was cooled to -78 ºC. Two equivalents of PMe_3 were added and the solution was allowed to warm until the blue solution turned to a green color. The solution was recooled to -78 ºC, then transferred to a precooled IR cell via a precooled syringe (both at -78 ºC). The color changes observed are the same as occur in synthetic scale reactions.

$(C_5Ph_5)Cr(CO)_2PMe_3$•THF (2). $(C_5Ph_5)Cr(CO)_3$•C_6H_6 (0.50 g, 0.76 mmol) was dissolved in 10 mL THF. The solution was then cooled to -78 ºC and 0.21 mL PMe_3 (2.0 mmol) was added. The solution was allowed to warm to room temperature with stirring (*ca*. 1 h). As the dark blue solution warmed it initially turned a jade green color, then deep cherry-red. The solution was filtered via cannula and layered with 12 mL of hexane to yield **2** (0.48 g, 0.76 mmol) in 88% yield as dark red crystals: mp 211-218 ºC (dec); ^1H NMR (C_6D_6) δ 7.32 (m, C_5Ph_5, br) 5.76 (s, PMe_3, br); visible λ_{max} (CH_2Cl_2) 516 nm. Anal. Calcd for $C_{44}H_{42}CrO_3P$: C, 75.31; H, 6.03. Found: C, 75.69; H, 5.79.

$(C_5Ph_5)Cr(CO)_2PMe_2Ph$•THF (3). $(C_5Ph_5)Cr(CO)_3$•C_6H_6 (0.50 g, 0.76 mmol) was dissolved in 10 mL THF and 0.50 mL PMe_2Ph (3.7 mmol) was added. The solution was stirred overnight. The resulting red solution was filtered via cannula and layered with 12 mL of hexane to yield **3** (0.48 g, 0.76 mmol) in 72% yield as dark red crystals: mp 198-200 ºC (dec); ^{1}H NMR (C_6D_6) δ 7.18 (m, C_5*Ph*$_5$ and P(Me$_2$*Ph*)$_3$, br), 5.49 (s, P(*Me*$_2$Ph)$_3$, br); visible λ_{max} (CH_2Cl_2) 470 nm (sh). Anal. Calcd for $C_{49}H_{44}CrO_3P$: C, 77.05; H, 5.81. Found: C, 76.54; H, 5.50.

(C_5Ph_5)Cr(CO)$_2$P(OMe)$_3$•THF (4). The procedure is the same as for **2** except that a magenta colored product is obtained in 90% yield: mp 188-192 ºC (dec); ^{1}H NMR (C_6D_6) δ 7.34 (m, C_5*Ph*$_5$, br), 5.32 (s, P(O*Me*)$_3$, br); visible λ_{max} (CH_2Cl_2) 532 nm. Anal. Calcd for $C_{44}H_{42}CrO_6P$: C, 70.49; H, 5.65. Found: C, 71.05; H, 5.06.

Results and Discussion

Syntheses. Reaction of the (C_5Ph_5)Cr(CO)$_3$ radical with a variety of neutral, monodentate Lewis bases resulted in substitution products or no reaction between the materials depending on the ligand. The small, soft ligands PMe_3 and P(OMe)$_3$ react with (C_5Ph_5)Cr(CO)$_3$ in THF solution at low temperatures to yield the substitution products, (C_5Ph_5)Cr(CO)$_2$L (eq 1) as highly colored, crystalline materials in high yields (compounds **2** and **4**, respectively). PMe_2Ph reacts

$$(C_5Ph_5)Cr(CO)_3 + L \xrightarrow[\text{THF}]{-78\ ^\circ\text{C}} (C_5Ph_5)Cr(CO)_2L + CO \qquad (1)$$

with **1** at ambient temperature to yield this product (**3**) in slighly lower yields. The former reactions proceed very rapidly at ambient temperature, however isolated yields of the products are somewhat reduced. Unlike for $CpMn(CO)_3^+$,[6,13] no evidence for disubstitution of **1** was observed. All are air-sensitive, both in solution and in the solid state. ^{1}H NMR spectra were very broad and no resonances were observed in ^{31}P NMR spectra of these compounds.

Infrared spectral and electrochemical data for these complexes are collected in Tables 5 and 6, respectively. A cyclic voltammogram of **2** is presented in Figure 1. The CO stretching frequencies and complex reduction potentials both follow the expected trends for the ligands. Two aspects of the electrochemical data are noteworthy. Replacing Cp by C_5Ph_5 in a complex usually results in potential shifts of *ca*. 0.2 V to more positive values.[4,14] In contrast, the -1/0 couples for the PMe_3 and PMe_2Ph complexes show roughly the opposite trend. Hershberger and

Kochi examined a variety of (MeCp)Mn$(CO)_2$L complexes by cyclic voltammetry and found that replacing CO by PEt_3 and $P(OMe)_3$, resulted in potential shifts of -0.70 V and -0.42 V, respectively.[15] For complexes **2** and **4** the shifts are -0.85 V and -0.54 V, respectively. Thus, the shifts in the reduction potentials of **2** and **4** relative to **1** are consistent with precedent. At ambient temperature, each complex also undergoes an irreversible oxidation approximately 1.3 V to more positive potential than the reversible reduction. The anodic waves equaled the cathodic waves in height within 20% in all cases and are also assigned as one-electron processes.

A low temperature (-78º) infrared spectrum of the reaction mixture of **1** with excess PMe_3 shows 4 absorptions (Table 5). The spectrum is consistent with a compound of the formula $[(C_5Ph_5)Cr(CO)_3PMe_3][(C_5Ph_5)Cr(CO)_3]$.[16,17] It is well established that 17e complexes tend to undergo substitution reactions via associative pathways.[2d,7] Thus, a plausible reaction mechanism is shown in eq (2) and (3). When the reaction mixture is warmed to ambient temperature, **2** is produced quantitatively (eq 4). Further studies of this and similar low temperature reactions are underway.

$$(C_5Ph_5)Cr(CO)_3 + PMe_3 \xrightarrow{-78\ ^\circ C} (C_5Ph_5)Cr(CO)_3PMe_3 \qquad (2)$$

$$(C_5Ph_5)Cr(CO)_3PMe_3 + (C_5Ph_5)Cr(CO)_3 \xrightarrow{-78\ ^\circ C} [(C_5Ph_5)Cr(CO)_3PMe_3][(C_5Ph_5)Cr(CO)_3] \qquad (3)$$

$$[(C_5Ph_5)Cr(CO)_3PMe_3][(C_5Ph_5)Cr(CO)_3] \xrightarrow{PMe_3} 2\ (C_5Ph_5)Cr(CO)_2PMe_3 + 2\ CO \qquad (4)$$

$PMePh_2$ reacts with **1** at ambient temperature to yield solutions which display CO absorptions in the infrared where expected, but from which very little substitution product can be isolated. The following ligands do not react with **1** even at elevated temperatures (e.g. refluxing THF or benzene): PPh_3, $P(OPh)_3$, 2, 2'-bipyridine, and PhC≡CPh. The data for PMe_3, PMe_2Ph, and $PMePh_2$ suggest that steric effects are probably very important in the lack of reactivity of PPh_3 and $P(OPh)_3$.

Molecular Structure of $(C_5Ph_5)Cr(CO)_2PMe_3$•0.5THF. The X-ray crystal structure of $(C_5Ph_5)Cr(CO)_2PMe_3$•0.5THF is displayed in Figure 2. Bond distances and angles are listed in Tables 2 and 3, respectively. Phenyl dihedral angles are given in Table 4. There are two conformers in the unit cell that do not differ in any chemically significant way. As in other, similar paramagnetic systems, the tripodal angles deviate significantly from 90°.[4,9a,e] Fortier and coworkers have reported calculations describing the origin of this effect.[9e] The P atom lies below a C-C bond of the C_5 ring (a staggered conformation). $Cp^*Cr(CO)_2PMe_3$,[9e] also adopts a staggered conformation, but for $CpCr(CO)_2PPh_3$[9a] the P atom eclipses a carbon atom of the C_5 ring. As we will show below, the conformational energy difference for **2** is small, less than or on the order of *k*T at 200 K (0.02 eV). One further feature of the structure warrants comment. Elemental analysis, ^{1}H NMR, and thermogravimetric analysis[18] all support formulation of the solid phase as a monosolvate. Since all atoms in this structure were at full occupancy, it is likely that the structure was obtained of a rare crystal of an unrepresentative solvation number.

ESR Spectra. ESR spectra of **2**, **3**, and **4** in frozen toluene solution are rhombic with three distinct *g*-components. Spectra of **2** and **3** are shown in Figures 3 and 4. The spectrum of **4** is very similar to that of **2**. Interpretation of the spectra is straightforward, and the resulting parameters are given in Table 7(a). In all cases, the low-field features (g_{max}) are much broader than those corresponding to the two smaller *g* components. For **2** and **4**, the low-field features increase in width with increasing temperature whereas in spectra of **3**, these features are not as broad and sharpen slightly with increasing temperature. Spectra of **4** in dcm/dce were essentially identical to those in toluene except that the low-field features were broader and could not be located accurately, even at 125 K. These linewidth effects will be discussed elsewhere.[19]

The *g*-matrices have one component close to the free-electron *g*-value, g_e, a second component slightly larger than g_e, and a third component substantially larger than g_e. This pattern is characteristic of low-spin d^5 systems[11] and can be understood qualitatively in terms of a simple ligand-field theory model. The degeneracy of the octahedral ligand-field configuration, t_{2g}^5, is lifted in lower symmetry, but strong spin-orbit coupling of the singly-occupied orbital (SOMO) with the other two components of the t_{2g} set leads to two *g*-components greater than g_e; the third *g*-component differs from g_e through spin-orbit coupling with one of the e_g orbitals which is empty and at much higher energy. Although the spectra of $(C_5Ph_5)Cr(CO)_2L$ fit this qualitative pattern, they exhibit a temperature-dependent linewidth effect which requires a more detailed analysis. Furthermore, the spectra in liquid solution at low temperatures are not isotropic but resemble the frozen solution spectra, albeit with significant shifts in the positions of features.

The complexes $(C_5Ph_5)Cr(CO)_2L$ have nominal C_s symmetry so that the SOMO could belong to either the a' or a'' representation. Previous work on related systems[9e,20,21] and extended Hückel MO calculations[19] suggest a SOMO of a'' symmetry. Taking xz as the plane of symmetry, the SOMO is given by eq (5).

$$|\mathrm{SOMO}\rangle = a_1|\mathrm{xy}\rangle + a_2|\mathrm{yz}\rangle + \ldots \tag{5}$$

Components of the g-matrix are given by eqs (6)[11] where, for example, $\delta_{x^2-y^2}$ is given

$$g_{xx} = g_e + 2[a_1^2\delta_{xz} + a_2^2(\delta_{x^2-y^2} + 3\delta_{z^2})] \tag{6a}$$

$$g_{yy} = g_e + 2(a_1^2\delta_{yz} + a_2^2\delta_{xy}) \tag{6b}$$

$$g_{zz} = g_e + 2(4a_1^2\delta_{x^2-y^2} + a_2^2\delta_{xz}) \tag{6c}$$

$$g_{xz} = -2a_1a_2(\delta_{xz} + 2\delta_{x^2-y^2}) \tag{6d}$$

by eq (7), in which ζ_{Cr} is the spin-orbit coupling constant for Cr, $E_0 - E_k$ is the energy of the kth

$$\delta_{x^2-y^2} = \zeta_{Cr}\sum_{k\neq 0}\frac{c_{k,x^2-y^2}^2}{E_0 - E_k} \tag{7}$$

MO relative to the energy of the SOMO, and c_{k,x^2-y^2} is the LCAO coefficient of $d_{x^2-y^2}$ in the kth MO. EHMO calculations[19] suggest that the two highest doubly-occupied MO's, just below the SOMO in energy (the other members of the t_{2g} set), are predominantly $d_{x^2-y^2}$ and d_{z^2} in character so that $\delta_{xz}, \delta_{yz}, \delta_{xy} << \delta_{x^2-y^2}, \delta_{z^2}$; Thus g_{yy} is expected to be close to g_e, but the other components should be larger. The g-matrix is diagonalized by rotation about the y-axis by the angle β, given by eq (8), where $R = a_2/a_1$ and $Q = \delta_{z^2}/\delta_{x^2-y^2}$.

$$\tan 2\beta = \frac{-4R}{4 - R^2(1 + 3Q)} \tag{8}$$

The X and Z principal values of the g-matrix then are given by eq (9). Since experimentally, g_X is

$$g_{XZ} = g_e + a_1^2 \delta_{x^2-y^2} \left[4 + R^2 (1 + 3Q)\right] \left\{ 1 \pm \sqrt{1 - \frac{48 R^2 Q}{\left[4 + R^2 (1 + 3Q)\right]^2}} \right\} \tag{9}$$

close to g_e and g_Z is much larger than g_e, the square root term of eq (9) is apparently close to 1.[22] Spectra in liquid solution 10-20 K above the melting point of the solvent appear as approximately axial powder patterns. Spectra of **2** and **3** are shown in Figures 3 and 4; again the spectrum of **4** is qualitatively similar to that of **2**, with features significantly sharper than for **3**. In all cases, the features broaden at higher temperatures and eventually coalesce into a single broad line. Although the line narrows somewhat near room temperature, ^{31}P splitting is never resolved. Parameters for the approximately axial spectra are given in Table 7(b).

The parallel features in the axial spectra are shifted upfield from the frozen solution g_Z features and the perpendicular features are close to the position of the g_Y features of the frozen solution spectra. At temperatures just above the melting point, the viscosity of toluene or dce/dcm is high, and it is not surprising that molecular rotation is too slow to produce an isotropic spectrum. Apparently there is some degree of averaging, however, such that the g_X and g_Y features are merged and the g_Z features somewhat shifted. The most likely explanation of this behavior is that the $Cr(CO)_2L$ moiety is nearly freely rotating relative to the C_5Ph_5 group. In other words, the very bulky "seat" of the "piano stool" is essentially stationary on the ESR time scale while the "legs" rotate freely. The bulkier PMe_2Ph ligand would be expected to impede this averaging process, and features in the approximately axial spectra of **3** are significantly broader than those of **2** or **4**.

This behavior can be simulated using the program described by Schneider and Freed.[23] Shown in Figure 5 are computer simulations using the spin Hamiltonian parameters for **2** and a 5-Gauss Lorentzian linewidth. For the simulations in Figure 5a, isotropic rotational diffusion is assumed with $D_x = D_y = D_z$ ranging from 10^7 to 5×10^8 s^{-1} whereas in Figure 5b, rotational diffusion is anisotropic with $D_x = D_y = 10^6$ s^{-1} and D_z ranging from 10^7 to 5×10^8 s^{-1}. Although isotropic rotational diffusion can lead to an approximately axial spectrum, the parallel features are very broad and both the parallel and perpendicular features shift significantly from the frozen solution positions. We can obtain an order-of-magnitude estimate of the isotropic rotational diffusion coefficients from eqs (10). Extrapolating literature values of the viscosity of

$$D = 1/6\tau_r \tag{10a}$$

$$\tau_r = V_h\eta/kT \tag{10b}$$

toluene[24] to 200 K, we obtain $\eta \approx 0.43$ kg m^{-1}s^{-1}. Assuming that **2** is approximately spherical with a radius of about 7 Å, $\tau_r \approx 2 \times 10^{-7}$ s, $D \approx 7 \times 10^5$ s^{-1}, about two orders of magnitude slower than required to obtain an approximately axial spectrum from isotropic motion.

On the other hand, anisotropic rotational diffusion with $D_x = D_y \ll D_z \approx 2 \times 10^8$ s^{-1} gives a reasonable account of the experimental results. This rate is considerably faster than might have been expected for rotational diffusion of the $Cr(CO)_2PMe_3$ moiety in toluene at 200 K, ($D_z \approx 3 \times 10^7$ s^{-1}, assuming a volume about 1/10 that of the whole complex and accounting for rotation about one axis). The most likely explanation is that the "piano-stool legs" rotate in a nearly solvent-free cavity created by the C_5Ph_5 ligand.

Assuming that anisotropic rotational diffusion is fast enough to completely average g_x and g_y, that the parallel axis corresponds to the Cr–Cp vector (the z-axis) and that the Z principal axis of the g-matrix differs from this axis by the angle β, the parallel and perpendicular components of the averaged g-matrix are given by eqs (11). These equations were used to compute the values of

$$2g_{\|}^2 = g_Z^2 + g_X^2 + (g_Z^2 - g_X^2)\cos^2 2\beta \tag{11a}$$

$$4g_{\perp}^2 = g_Z^2 + g_X^2 + 2g_Y^2 - (g_Z^2 - g_X^2)\cos^2 2\beta \tag{11b}$$

β listed in Table 8. Except for **4**, the agreement between values of β computed from $g_{\|}$—eq (11a)—and those computed from $g_{\perp}$—eq (11b)—is quite good, suggesting that the model is at least qualitatively correct. Extended Hückel MO calculations[19] suggest that $Q \approx 1.4$; with this value, $\beta = 16^{\circ}$ and eq (8) give $R = -0.46$, in reasonable agreement with the EHMO prediction of 0.34. The values of beta listed in Table 8 also may be compared with those obtained from ESR studies of $CpCr(CO)_2PPh_3$[9c] and $(C_5Me_5)Cr(CO)_2PMe_3$[9e] diluted into single crystals of the Mn analogs. For $CpCr(CO)_2PPh_3$, four paramagnetic sites were found with slightly different principal values of the *g*-matrix and beta ranging from 3 to 8º; for $(C_5Me_5)Cr(CO)_2PMe_3$, only one site was found with beta = 2.4º. These angles refer to the orientation of the g_{max} principal axis relataive to the Mn-CNT axis in the host crystal and so may not be exactly equal to those relative to the Cr-CNT axis. Nonetheless, the angles are considerably smaller than those found in the present work; whether this reflects an error in our analysis or a true difference between the C_5Ph_5 ligand and the Cp and C_5Me_5 ligands is unclear.

Acknowledgments. The research at Marshall University was supported by the National Science Foundation (Grant NSF CHE-9123178) and the donors of The Petroleum Research Fund, administered by the American Chemical Society. The NSF provided funds towards the University of Delaware diffractometer. We thank Dr. R. J. Hoobler and Prof. J. W. Larson for experimental assistance, Dr. Michael Iglehart for obtaining and interpreting the TGAs, Prof. W. E. Geiger for helpful suggestions regarding both electrochemical experiments and interpretation of our results, Prof. J. H. Freed and Dr. R. Crepeau for supplying the ESR simulation program, and Prof. M. B. Zimmt for assistance in implementing the program at Brown.

Supporting Information Available. For $(C_5Ph_5)Cr(CO)_2PMe_3$•0.5THF as follows: Table 1S, atomic coordinates and equivalent isotropic displacement coefficients, Table 2S, anisotropic displacement coefficients, Table 3S, hydrogen-atom coordinates, and a TGA of **2** (12 pages). Ordering information is given on any current masthead page.

References

(1) (a) Marshall University. (b) University of Delaware. (c) Brown University.

(2) (a) Connelly, N. G.; Geiger, W. C. *Adv. Organomet. Chem.* **1984**, *23*, 1. (b) Baird, M. C. *Chem. Rev.* **1988**, *88*, 1217. (c) Astruc, D. *Chem. Rev.* **1988**, *88*, ll89. (d) *Organometallic Radical Processes*; Trogler, W. C., Ed.; Elsevier: Amsterdam, 1990.

(3) (a) Adams, R. D.; Collins, D. E.; Cotton, F. A. *J. Am. Chem. Soc.* **1974**, *96*, 749. (b) McLain, S. J. *J. Am. Chem. Soc.* **1988**, *110*, 643. (c) Goh, L. Y.; Khoo, S. K.; Lim, Y. Y. *J. Organomet. Chem.* **1990**, *399*, 115. (d) Goh, L. Y.; Hambley, T. W.; Darensbourg, D. J.; Reibenspies, J. *J. Organomet. Chem.* **1990**, *381*, 349. (e) Watkins, W. C.; Jaeger, T.; Kidd, C. E.; Fortier, S.; Baird, M. C.; Kiss, G.; Roper, G. C.; Hoff, C. D. *J. Am. Chem. Soc.* **1992**, *114*, 907. (f) The fluorenyl complex $(C_{13}H_9)Cr(CO)_3$ has also been prepared. It is also unstable and undergoes a $Cr(CO)_3$ shift from the C_5 ring to a C_6 ring, followed by a dimerization through the methine C_5 carbon. Novikova, L. N.; Ustynyuk, N. A.; Tumanskii, B. L.; Petrovskii, P. V.; Borisenko, A. A.; Kukharenko, S. V.; Strelets, V. V. *Isv. Akad. Nauk, Ser. Khim.* **1995**, 1354 (Engl. Transl. *Russ. Chem. Bull*. **1995**, *44*, 1306).

(4) Hoobler, R. J.; Hutton, M. A.; Dillard, M. M.; Castellani, M. P.; Rheingold, A. L.; Rieger, A. L.; Rieger, P. H.; Richards, T. C.; Geiger, W. E. *Organometallics* **1993**, *12*, 116.

(5) (a) Kochi, J. K. *Organometallic Mechanisms and Catalysis*; Academic; New York, 1978, Chap. 8. (b) Ref. 2d, Chap. 4 and 9.

(6) Huang, Y.; Carpenter, G. B.; Sweigart, D. A.; Chung, Y. K.; Lee, B. Y. *Organometallics* **1995**, *14*, 1423.

(7) (a) Atwood, J. D. *Inorganic and Organometallic Reaction Mechanisms*; Brooks/Cole: Monterey, 1985; p 123. (b) Crabtree, R. H. *The Organometallic Chemistry of the Transition Metals*; John Wiley and Sons: New York, 1988; pp 80-81.

(8) (a) Therien, M. J.; Trogler, W. C. *J. Am. Chem. Soc.* **1988**, *110*, 4942. (b) Lin, Z.; Hall, M. B. *Inorg. Chem.* **1992**, *31*, 2791.

(9) (a) Cooley, N. A.; Watson, K. A.; Fortier, S.; Baird, M. C. *Organometallics* **1988**, *7*, 2563. (b) Cooley, N. A.; MacConnachie, P. T. F.; Baird, M. C. *Polyhedron* **1988**, *7*, 1965. (c) Cooley, N. A.; Baird, M. C.; Morton, J. R.; Preston, K. F.; Le Page, Y. *J. Magn. Reson.* **1988**, *76*, 325. (d) Watkins, W. C.; Macartney, D. H.; Baird, M. C. *J. Organomet. Chem.* **1989**, *377*, C52. (e) Fortier, S.; Baird, M. C.; Preston, K. F.; Morton, J. R.; Ziegler, T.; Jaeger, T. J.; Watkins, W. C.; MacNeil, J. H.; Watson, K. A.; Hensel, K.; Le Page, Y.; Charland, J.-P.; Williams, A. J. *J. Am. Chem. Soc.* **1991**, *113*, 542. (f) O'Callaghan, K. A. E..; Brown, S. J.; Page, J. A.; Baird, M. C.; Richards, T. C.; Geiger, W. E. *Organometallics* **1991**, *10*, 3119. (g) Watkins, W. C.; Hensel, K.; Fortier, S.; Macartney, D. H.; Baird, M. C.; McLain, S. J. *Organometallics* **1992**, *11*, 2418.

(10) Jaeger, T. J.; Baird, M. C. *Organometallics* **1988**, *7*, 2074.

(11) Rieger, P. H. *Coord. Chem. Rev.* **1994**, *135*, 203.

(12) Solutions at higher concentrations than normal were used because of the high air-sensitivity of the complexes in solution. Under the conditions employed, 0.5 mM solutions rarely maintained their integrity for more than a few minutes. Typical values of ΔE_p were in the range 150 - 180 mV. A 3 mM solution of $(C_5Ph_5)Cr(CO)_3$ gave the same $E^o(0/1\text{-})$ value as that reported for a much more dilute solution.[4]

(13) It is interesting that Baird and coworkers do not report observing evidence of disubstitution reactions occurring in isoelectronic $CpCr(CO)_3$.[6] While the large size of the C_5Ph_5 ligand probably precludes disubstitution in **1** for the ligands studied here, Baird's work suggests that a steric argument may not be necessary.

(14) (a) Broadley, K.; Lane, G. A.; Connelly, N. G.; Geiger, W. E. *J. Am. Chem. Soc.* **1983**, *105*, 2486. (b) Connelly, N. G.; Geiger, W. E.; Lane, G. A.; Raven, S. J.; Rieger, P. H. *J. Am. Chem. Soc.* **1986**, *108*, 6219. (c) Lane, G. A.; Geiger, W. E.; Connelly, N. G. *J. Am. Chem. Soc.* **1987**, *109*, 402. (d) Connelly, N. G.; Manners, I. *J. Chem. Soc., Dalton Trans.* **1989**, 283.

(15) Hershberger, J. W.; Kochi, J. K. *Polyhedron* **1983**, *2*, 929.

(16) Two absorptions, 1892 and 1791 cm^{-1}, are associated with $(C_5Ph_5)Cr(CO)_3^-$.[4] The infrared spectrum of this complex is qualitatively similar to $[(C_5Ph_5)Cr(CO)_2(depe)]$-$[(C_5Ph_5)Cr(CO)_3]$ (Jarrell, C. S.; Castellani, M. P. unpublished results).

(17) To our knowledge no such Cr complexes are known, however, several similar Mo complexes have been isolated. The infrared spectra of the Mo complexes are very similar to those obtained for the Cr system. (a) Nolte, M. J.; Reimann, R. H. *J. Chem. Soc., Dalton Trans.* **1978**, 932. (b) Asdar, A.; Tudoret, M.-J.; Lapinte, C. *J. Organomet. Chem.* **1988**, *349*, 353.

(18) A TGA of this compound shows that the complex loses its THF solvate well before decomposition begins. Desolvation begins at *ca*. 150 ºC and results in the crystals losing their luster with no significant decoloration occuring. Complexes **3** and **4** undergo similar visual changes for, presumably, the same reason. A copy of the TGA of **2** is provided in the Supplementary Material.

(19) Castellani, M. P.; Connelly, N. G.; Rieger, A. L.; Rieger, P. H. to be published.

(20) Morton, J. R.; Preston, K. F.; Cooley, Baird, M. C.; Krusic, P. J.; McLain, S. J. *J. Chem. Soc., Faraday Trans. I* **1987**, *83*, 3535.

(21) Pike, R. D.; Rieger, A. L.; Rieger, P. H. *J. Chem. Soc., Faraday Trans. I* **1989**, *85*, 3913.

(22) Since EHMO calculations[19] suggest that R is negative and Q is positive, eq (9) predicts g_Z, $g_X > g_e$. The observed values of g_X, *ca*. 1.994, suggest that the δ_{xz} terms in eqs (6) are not entirely negligible.

(23) Schneider, J. H.; Freed, J. H. in *Spin Labeling: Theory and Application, Biological Magnetic Resonance, Vol. 8*, Berliner, L. J.; Reuben, J., eds, Plenum, New York, 1989.

(24) *International Critical Tables*, Vol. VII, Washburn, E. W. ed, McGraw-Hill, New York, 1926-1930, p 218.

(25) Nicholson, R. S. *Anal. Chem.* **1966**, *38*, 1406.

Table 1. Crystal and Refinement Data for $(C_5Ph_5)Cr(CO)_2PMe_3$•0.5THF

a. Crystal Data

formula	$C_{40}H_{34}CrO_2P$
fw	629.6
cryst system	Triclinic
space group	$P\bar{1}$
a, Å	12.834(2)
b, Å	13.271(3)
c, Å	22.536(5)
α, deg	90.96(2)
β, deg	94.29(2)
γ, deg	112.55(1)
V, $Å^3$	3530.6(12)
Z	4
color	dark red
crystal size, mm	0.44 x 0.58 x 0.74
D (Calcd), g/cm^3	1.185
abs coeff, cm^{-1}	0.401 mm^{-1}

b. Data Collection

diffractometer	Siemens P4
radiation	MoKα (λ =0.710 73 Å)
temp, K	293
2θ scan range, deg	1.00°
scan type	Wycoff
reflns collcd	14234
obsd rflns	6465 ($F > 5.0\sigma(F)$)

c. Solution and Refinement

solution	direct methods
refinement method	full-matrix least-squares
quantity minimized	$\Sigma w(F_o - F_c)^2$
weighting scheme	$w^{-1} = \sigma^2(F) + 0.0015F^2$
number of parameters refined	838
final *R* indices (obs. data),%	*R* = 5.62, w*R* = 6.67
R indices (all data), %	*R* = 12.75, w*R* = 8.93
GOF	1.11
data-to-parameter ratio	7.7:1
largest difference peak, eÅ^{-3}	0.34
largest difference hole, eÅ^{-3}	-0.39

Table 2. Selected Bond Distances (Å) in $(C_5Ph_5)Cr(CO)_2PMe_3$•0.5THF

	conformer A	conformer B
Cr-C(1)	2.254(5)	2.269(5)
Cr-C(2)	2.288(5)	2.256(4)
Cr-C(3)	2.241(6)	2.236(5)
Cr-C(4)	2.198(7)	2.212(5)
Cr-C(5)	2.218(6)	2.221(4)
Cr-CNT[a]	1.881	1.881
Cr-C(6)	1.837(6)	1.836(7)
Cr-C(7)	1.834(6)	1.812(7)
Cr-P	2.383(2)	2.372(2)
C(1)-C(2)	1.430(7)	1.424(7)
C(2)-C(3)	1.441(8)	1.425(8)
C(3)-C(4)	1.425(6)	1.430(7)
C(4)-C(5)	1.429(8)	1.432(8)
C(1)-C(5)	1.429(7)	1.429(8)
C(6)-O(6)	1.162(7)	1.156(9)
C(7)-O(7)	1.149(8)	1.158(9)

[a]CNT = centroid of the cyclopentadienyl ring

Table 3. Bond Angles (º) in $(C_5Ph_5)Cr(CO)_2PMe_3$•0.5THF

	conformer A	conformer B
C(6)-Cr-C(7)	78.7(3)	78.0(4)
P-Cr-C(6)	89.4(2)	86.9(2)
P-Cr-C(7)	89.8(2)	90.4(2)
OC-Cr-CO (avg)	175.8(6)	176.8(7)
C(6)-Cr-CNT[a]	125.8	124.8
C(7)-Cr-CNT	122.4	126.1
P-Cr-CNT	134.8	133.3

[a]CNT = centroid of the cyclopentadienyl ring

Table 4. Phenyl Ring Torsion Angles (deg) in $(C_5Ph_5)Cr(CO)_2PMe_3$•0.5THF

Cp Carbon	conformer A	conformer B
1	51.9	47.7
2	48.0	55.6
3	51.1	45.6
4	54.7	56.8
5	50.0	55.0

Table 5. Infrared Spectral Data for $(C_5Ph_5)Cr(CO)_2L$ Complexes

complex	solvent	ν(C≡O), $cm^{-1,a}$	reference
$(C_5Ph_5)Cr(CO)_3$	THF	2005, 1897	4
$(C_5Ph_5)Cr(CO)_2PMe_3$	THF	1911, 1797	this work
$CpCr(CO)_2PMe_3$	CH_2Cl_2	1910, 1778	9f
$(C_5Ph_5)Cr(CO)_2PMe_2Ph$	THF	1911, 1792	this work
$(C_5Ph_5)Cr(CO)_2P(OMe)_3$	THF	1923, 1816	this work
$[(C_5Ph_5)Cr(CO)_3PMe_3][(C_5Ph_5)Cr(CO)_3]$[b]	THF	2025, 1956, 1892, 1791	this work

[a]Absorptions are strong unless otherwise stated.

[b]Spectrum taken at -78 ºC.

Table 6. Electrochemical Data for $(C_5Ph_5)Cr(CO)_2L$ in CH_2Cl_2

complex	$E_{pa}(0/1+)$ (V)[a, b]	$E^o(0/1-)$ (V)[a]	i_{pa}/i_{pc}[c]	reference
$(C_5Ph_5)Cr(CO)_3$	*ca* . 0.9[e]	-0.69	1.0	4
$(C_5H_5)Cr(CO)_2PMe_3$	-----	-1.42	-----	9f
$(C_5Ph_5)Cr(CO)_2PMe_3$[d]	-0.07	-1.56	0.98	this work
$(C_5H_5)Cr(CO)_2PMe_2Ph$	-0.37	-1.36	-----	9f
$(C_5Ph_5)Cr(CO)_2PMe_2Ph$[d]	-0.06	-1.48	0.86	this work
$(C_5Ph_5)Cr(CO)_2P(OMe)_3$[d]	0.05	-1.26	0.95	this work

[a]Potential *vs* Fc.

[b]Irreverisible.

[c]Determined according to ref. 25.

[d]Scan rate 100 mV/s; 0.1 M $(^nBu_4N)PF_6$; *ca*. 3 mM complex.

[e]Appears as a very broad peak. This work

Table 7. ESR Parameters for $(C_5Ph_5)Cr(CO)_2L$.

(a) Frozen Solution Spectra.

L	*T*/K (solvent)	g_1	g_2	g_3	A_1[a]	A_2[a]	A_3[a]
PMe_3 (**2**)	125-160 (toluene)	1.9941(3)	2.0130(3)	2.104(2)	34.2(2)	35.8(4)	34(1)
PMe_2Ph (**3**)	105-120 (toluene)	1.9940(2)	2.0130(2)	2.1060(2)	32.6(2)	34.8(2)	34.2(2)
$P(OMe)_3$ (**4**)	125-145 (toluene)	1.9944(3)	2.0147(5)	2.130(3)	40.4(2)	45.9(2)	35(2)
$P(OMe)_3$ (**4**)	125-160 (dcm/dce)	1.9940(2)	2.0140(2)	b	40.2(3)	45.5(2)	b

(b) Liquid Solution Spectra.

L	*T*/K (Solvent)	$g_\perp$	$g_\parallel$	$A_\perp$[a]	$A_\parallel$[a]
PMe_3 (**2**)	200 K (toluene)	2.012(1)	2.090(1)	35(1)	35(1)
PMe_2Ph (**3**)	190 K (toluene)	2.011(1)	2.091(1)	36(1)	32(2)
$P(OMe)_3$ (**4**)	180-195 K (toluene)	2.006(2)	2.112(1)	46(3)	45(1)
$P(OMe)_3$ (**4**)	185 K (dcm/dce)	2.012(1)	2.095(1)	45(1)	41(1)

[a] ^{31}P hyperfine coupling in units of 10^{-4} cm^{-1}.

[b] Features poorly resolved.

Table 8. Values of the angle β computed from axial spectra in toluene.

L	β [eq (11a)]	β [eq (11b)]	β (avg)
PMe_3	15.3 ± 1.0º	16.6 ± 1.3º	15.8 ± 0.6º
PMe_2Ph	15.7 ± 0.9º	15.4 ± 1.4º	15.6 ± 0.1º
$P(OMe)_3$	15.8 ± 1.0º	5.8 ± 4.8º	15.4 ± 2.0º

Figure Captions

Figure 1. Cyclic voltammogram of $(C_5Ph_5)Cr(CO)_2PMe_3$ (**2**). Scan rate 100 mV/s; 0.1 M $(^nBu_4N)PF_6$; *ca*. 3 mM complex in CH_2Cl_2.

Figure 2. Molecular structure and labeling scheme for $(C_5Ph_5)Cr(CO)_2PMe_3$•0.5THF (**2**).

Figure 3. ESR spectra of $(C_5Ph_5)Cr(CO)_2PMe_3$ (**2**) in toluene solution at 125, 165, and 200 K. The low-field portions of the 125 and 165 K spectra are shown magnified by a factor of 4.

Figure 4. ESR spectra of $(C_5Ph_5)Cr(CO)_2PMe_2Ph$ (**3**) in toluene solution at 120, 160, and 190 K.

Figure 5. Simulated spectra based on the spin Hamiltonian parameters of **2**: (a) Isotropic rotational diffusion with $D_x = D_y = D_z = D$; and (b) anisotropic rotational diffusion with $D_x = D_y = 10^6$ s^{-1} and $D_z = D$ = (i) 1×10^7, (ii) 2×10^7, (iii) 5×10^7, (iv) 1×10^8, and (v) 2×10^8 s^{-1}.

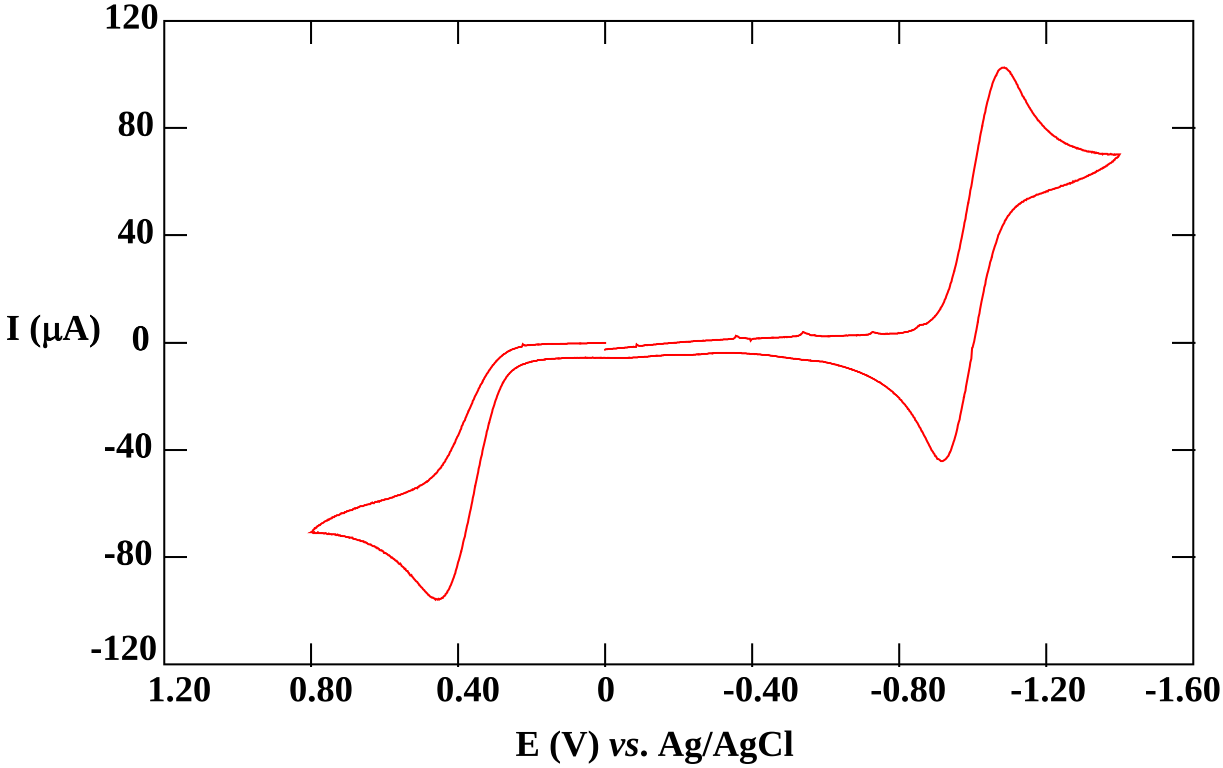

120
80
40
0
-40
-80
-120
I (μA)
1.20
0.80
0.40
0
-0.40
-0.80
-1.20
-1.60
E (V) *vs*. Ag/AgCl

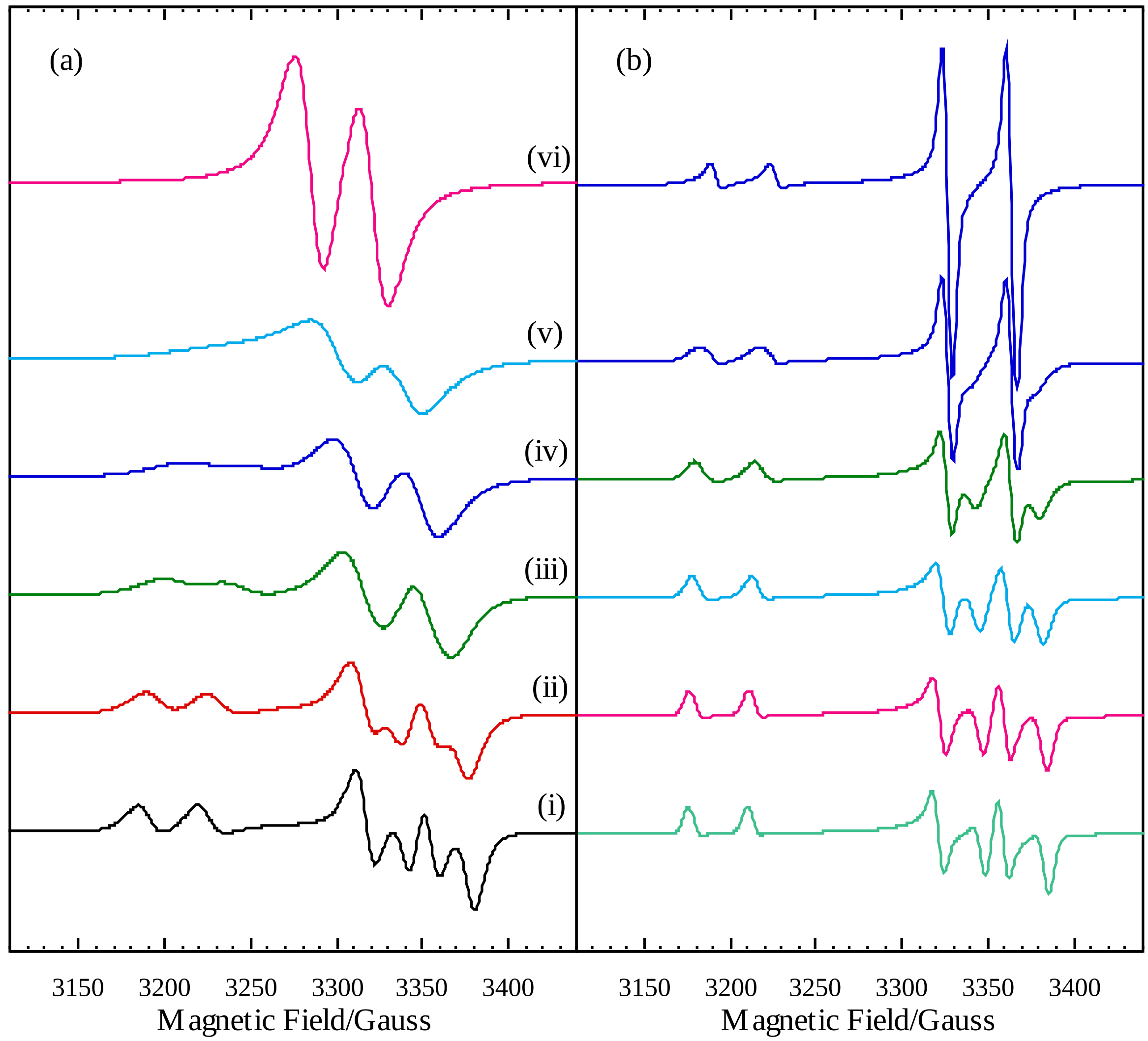
(a)
(b)
(vi)
(v)
(iv)
(iii)
(ii)
(i)
3150
3200
3250
3300
3350
3400
Magnetic Field/Gauss
3150
3200
3250
3300
3350
3400
Magnetic Field/Gauss

Supporting Information

for

Substitution Reactions of $(C_5Ph_5)Cr(CO)_3$: Structural, Electrochemical, and Spectroscopic Characterization of $(C_5Ph_5)Cr(CO)_2L$, L = PMe_3, PMe_2Ph, $P(OMe)_3$

by

D. John Hammack, Mills M. Dillard, Michael P. Castellani,* Arnold L. Rheingold,*

Anne L. Rieger, and Philip H. Rieger*

Table 1S. Atomic Coordinates (x10^4) and Equivalent Isotropic Displacement Coefficients ($Å^2$ x 10^3) for $(C_5Ph_5)Cr(CO)_2PMe_3$•0.5THF

	x	*y*	*z*	U^a
Cr	4760.8(7)	2519.2(7)	1403.6(4)	33(1)
P	3441(1)	3332(1)	1581.0(7)	47(1)
O(6)	6663(4)	4615(4)	1835(2)	74(2)
O(7)	5127(4)	2242(4)	2702(2)	73(3)
C(1)	4309(4)	1849(4)	452(2)	32(2)
C(2)	3799(4)	959(4)	822(2)	29(2)
C(3)	4693(4)	835(4)	1202(2)	30(2)
C(4)	5744(4)	1634(4)	1058(2)	33(2)
C(5)	5507(4)	2248(4)	589(2)	32(2)
C(6)	5926(6)	3816(5)	1649(3)	50(3)
C(7)	4941(5)	2341(5)	2205(3)	47(3)
C(8)	4056(7)	4705(6)	1888(4)	108(5)
C(9)	2528(7)	2654(7)	2149(4)	104(5)
C(10)	2430(7)	3497(7)	1028(3)	93(5)
C(11)	3049(5)	1448(5)	-492(2)	42(2)
C(12)	2603(5)	1778(6)	-999(3)	61(3)
C(13)	2846(6)	2865(7)	-1072(3)	64(3)
C(14)	3541(6)	3632(6)	-641(3)	62(3)
C(15)	3992(5)	3309(5)	-138(3)	47(3)
C(16)	3748(4)	2204(4)	-59(2)	33(2)
C(21)	1696(5)	517(5)	746(3)	50(3)
C(22)	585(5)	-247(6)	687(3)	62(3)
C(23)	352(5)	-1336(6)	662(3)	57(3)
C(24)	1235(5)	-1692(5)	681(3)	55(3)

C(25)	2344(5)	-934(5)	748(3)	45(3)
C(26)	2593(4)	176(4)	781(2)	32(2)
C(31)	3769(5)	-263(5)	2063(3)	48(3)
C(32)	3621(6)	-1119(5)	2435(3)	60(3)
C(33)	4253(6)	-1756(5)	2391(3)	67(3)
C(34)	5019(6)	-1552(5)	1971(3)	61(3)
C(35)	5175(5)	-696(4)	1592(3)	44(2)
C(36)	4543(4)	-46(4)	1631(2)	36(2)
C(41)	7265(5)	1748(5)	1865(3)	48(3)
C(42)	8297(6)	1691(6)	2036(3)	67(3)
C(43)	8994(6)	1609(6)	1619(3)	68(3)
C(44)	8639(5)	1551(5)	1016(3)	58(3)
C(45)	7602(5)	1581(5)	850(3)	45(3)
C(46)	6899(4)	1675(4)	1266(2)	33(2)
C(51)	6289(5)	2892(5)	-382(3)	46(3)
C(52)	7138(6)	3528(6)	-715(3)	64(4)
C(53)	8104(6)	4324(6)	-446(4)	70(4)
C(54)	8217(6)	4491(5)	162(4)	66(3)
C(55)	7370(5)	3857(5)	504(3)	50(3)
C(56)	6388(5)	3042(4)	236(2)	36(2)
Cr’	7100(1)	6890(1)	4046(1)	33(1)
P’	6725(1)	4997(1)	3948(1)	41(1)
O(6’)	6230(5)	6722(4)	2764(2)	109(3)
O(7’)	4648(4)	6411(5)	4076(3)	138(4)
C(1’)	8981(4)	7677(4)	4334(2)	27(2)
C(2’)	8367(4)	7563(4)	4846(2)	27(2)
C(3’)	7676(4)	8184(4)	4783(2)	29(2)

C(4’)	7854(4)	8682(4)	4221(2)	26(2)
C(5’)	8653(4)	8360(4)	3943(2)	29(2)
C(6’)	6590(6)	6791(5)	3255(3)	61(3)
C(7’)	5605(6)	6586(6)	4085(4)	77(4)
C(8’)	7487(6)	4662(5)	3382(3)	64(3)
C(9’)	5250(5)	4167(5)	3693(3)	74(3)
C(10’)	6916(6)	4204(5)	4570(3)	64(3)
C(11’)	10965(5)	8084(5)	4101(2)	40(2)
C(12’)	11893(5)	7800(5)	4054(3)	51(3)
C(13’)	11801(5)	6750(6)	4167(3)	56(3)
C(14’)	10821(5)	6006(5)	4335(3)	51(3)
C(15’)	9889(5)	6291(4)	4387(3)	41(2)
C(16’)	9944(4)	7331(4)	4263(2)	30(2)
C(21’)	9612(5)	7359(4)	5700(3)	40(2)
C(22’)	9762(5)	6979(5)	6255(3)	50(3)
C(23’)	8869(6)	6288(5)	6531(3)	58(3)
C(24’)	7783(5)	5943(5)	6243(3)	52(3)
C(25’)	7622(5)	6310(4)	5686(2)	40(2)
C(26’)	8520(4)	7030(4)	5410(2)	29(2)
C(31’)	7515(5)	8731(4)	5824(2)	39(2)
C(32’)	6981(5)	9083(5)	6246(3)	51(3)
C(33’)	5951(5)	9163(5)	6094(3)	52(3)
C(34’)	5464(5)	8885(5)	5523(3)	52(3)
C(35’)	5985(4)	8524(4)	5100(3)	40(2)
C(36’)	7029(4)	8446(4)	5244(2)	30(2)
C(41’)	7687(4)	10457(4)	4385(2)	34(2)
C(42’)	7395(5)	11317(4)	4198(3)	43(2)

C(43’)	6864(5)	11262(5)	3635(3)	46(3)
C(44’)	6610(5)	10345(5)	3268(3)	48(3)
C(45’)	6901(4)	9492(4)	3451(2)	39(2)
C(46’)	7455(4)	9548(4)	4013(2)	28(2)
C(51’)	9667(4)	9919(4)	3331(2)	38(2)
C(52’)	10206(5)	10365(5)	2834(3)	51(3)
C(53’)	10238(6)	9685(6)	2368(3)	66(4)
C(54’)	9748(6)	8572(6)	2413(3)	66(4)
C(55’)	9208(5)	8121(5)	2914(3)	52(3)
C(56’)	9164(4)	8799(4)	3378(2)	32(2)
O(1S)	8964(8)	5124(7)	8001(3)	127(4)
C(1S)	8509(8)	4149(8)	7683(5)	112(6)
C(2S)	9294(13)	3753(11)	7631(7)	249(13)
C(3S)	10284(11)	4412(14)	7943(9)	248(14)
C(4S)	10146(12)	5342(10)	8107(7)	179(9)

[a]Equivalent isotropic *U* defined as one third of the trace of the orthogonalized $\mathbf{U}_{ij}$ tensor.

Table 2S. Anisotropic Displacement Coefficients (Å^{2}x10^3).

	U_{11}	U_{22}	U_{33}	U_{12}	U_{13}	U_{23}
Cr	39(1)	34(1)	29(1)	19(1)	2(1)	2(1)
P	48(1)	44(1)	53(1)	24(1)	6(1)	-3(1)
O(6)	71(3)	56(3)	74(3)	4(3)	1(3)	-15(3)
O(7)	123(4)	76(3)	31(3)	52(3)	4(3)	7(2)
C(1)	38(3)	30(3)	30(3)	15(3)	1(2)	2(2)
C(2)	38(3)	30(3)	26(3)	20(2)	2(2)	1(2)
C(3)	37(3)	33(3)	26(3)	19(3)	8(2)	0(2)
C(4)	39(3)	33(3)	27(3)	15(3)	3(2)	0(2)
C(5)	39(3)	33(3)	29(3)	18(3)	6(2)	4(2)
C(6)	58(4)	52(4)	44(4)	26(4)	9(3)	1(3)
C(7)	67(4)	45(4)	38(4)	31(3)	6(3)	-1(3)
C(8)	77(6)	67(5)	181(9)	35(5)	-7(6)	-49(6)
C(9)	99(7)	133(8)	116(7)	73(6)	63(6)	51(6)
C(10)	103(6)	104(6)	105(7)	84(6)	-19(5)	-19(5)
C(11)	45(4)	48(4)	34(3)	20(3)	-4(3)	3(3)
C(12)	50(4)	82(5)	47(4)	24(4)	-6(3)	7(4)
C(13)	60(5)	92(6)	43(4)	34(4)	-9(3)	28(4)
C(14)	64(5)	69(5)	63(5)	36(4)	5(4)	30(4)
C(15)	54(4)	49(4)	42(4)	25(3)	-2(3)	6(3)
C(16)	35(3)	43(3)	27(3)	22(3)	5(2)	7(2)
C(21)	45(4)	54(4)	55(4)	25(3)	2(3)	-2(3)
C(22)	41(4)	82(5)	72(5)	32(4)	7(3)	-4(4)
C(23)	35(4)	67(5)	61(4)	10(3)	8(3)	3(4)
C(24)	45(4)	43(4)	64(4)	4(3)	5(3)	6(3)
C(25)	43(4)	42(4)	50(4)	16(3)	2(3)	2(3)

C(26)	34(3)	38(3)	27(3)	16(3)	2(2)	2(2)
C(31)	57(4)	50(4)	36(3)	19(3)	5(3)	6(3)
C(32)	68(5)	55(4)	43(4)	7(4)	3(3)	17(3)
C(33)	82(6)	44(4)	57(5)	6(4)	-10(4)	30(4)
C(34)	71(5)	40(4)	69(5)	22(3)	-21(4)	13(3)
C(35)	46(4)	39(3)	47(4)	16(3)	-4(3)	1(3)
C(36)	39(3)	34(3)	31(3)	10(3)	-3(3)	3(2)
C(41)	37(4)	61(4)	47(4)	19(3)	0(3)	12(3)
C(42)	58(5)	93(6)	52(4)	34(4)	-8(4)	16(4)
C(43)	38(4)	88(5)	80(6)	30(4)	-3(4)	18(4)
C(44)	47(4)	70(5)	71(5)	35(4)	11(4)	15(4)
C(45)	46(4)	53(4)	41(4)	26(3)	-1(3)	3(3)
C(46)	38(3)	32(3)	33(3)	18(3)	-1(3)	4(2)
C(51)	54(4)	55(4)	39(4)	28(3)	14(3)	13(3)
C(52)	76(5)	86(5)	48(4)	45(5)	27(4)	30(4)
C(53)	61(5)	74(5)	87(6)	35(4)	35(5)	43(5)
C(54)	53(4)	50(4)	94(6)	14(3)	21(4)	16(4)
C(55)	49(4)	45(4)	53(4)	14(3)	5(3)	6(3)
C(56)	44(4)	36(3)	35(3)	23(3)	4(3)	11(3)
Cr’	31(1)	27(1)	38(1)	10(1)	-2(1)	-2(1)
P’	45(1)	29(1)	46(1)	10(1)	1(1)	-1(1)
O(6’)	170(6)	62(4)	69(4)	29(4)	-63(4)	-3(3)
O(7’)	42(3)	111(5)	245(8)	18(3)	1(4)	-83(5)
C(1’)	26(3)	24(3)	30(3)	8(2)	4(2)	0(2)
C(2’)	20(3)	27(3)	30(3)	6(2)	0(2)	3(2)
C(3’)	20(3)	29(3)	35(3)	5(2)	1(2)	6(2)
C(4’)	26(3)	19(3)	32(3)	7(2)	0(2)	-3(2)

C(5')	34(3)	27(3)	24(3)	10(2)	1(2)	-1(2)
C(6')	73(5)	36(4)	60(5)	9(3)	-25(4)	1(3)
C(7')	31(4)	64(5)	127(7)	11(4)	2(4)	-42(4)
C(8')	71(5)	52(4)	69(5)	22(4)	14(4)	-16(4)
C(9')	56(5)	43(4)	109(6)	6(3)	-8(4)	-8(4)
C(10')	87(5)	37(4)	60(4)	15(4)	7(4)	16(3)
C(11')	40(3)	41(3)	41(3)	18(3)	5(3)	3(3)
C(12')	37(4)	63(4)	58(4)	22(3)	15(3)	13(3)
C(13')	44(4)	80(5)	61(4)	45(4)	9(3)	1(4)
C(14')	56(4)	41(4)	66(4)	29(3)	1(3)	6(3)
C(15')	33(3)	38(3)	52(4)	13(3)	5(3)	10(3)
C(16')	31(3)	34(3)	25(3)	15(3)	1(2)	-2(2)
C(21')	39(3)	34(3)	46(4)	12(3)	3(3)	7(3)
C(22')	48(4)	58(4)	47(4)	24(3)	-9(3)	6(3)
C(23')	79(5)	58(4)	47(4)	35(4)	9(4)	22(3)
C(24')	51(4)	60(4)	46(4)	20(3)	18(3)	23(3)
C(25')	36(3)	44(3)	38(3)	13(3)	8(3)	10(3)
C(26')	27(3)	30(3)	30(3)	12(2)	2(2)	0(2)
C(31')	42(3)	39(3)	38(3)	19(3)	6(3)	3(3)
C(32')	62(4)	53(4)	38(4)	22(3)	8(3)	-6(3)
C(33')	61(4)	48(4)	52(4)	21(3)	30(4)	3(3)
C(34')	41(4)	61(4)	64(5)	25(3)	22(3)	9(3)
C(35')	32(3)	44(3)	45(4)	14(3)	7(3)	1(3)
C(36')	31(3)	25(3)	35(3)	9(2)	10(2)	6(2)
C(41')	31(3)	33(3)	39(3)	14(3)	3(2)	4(3)
C(42')	41(3)	32(3)	59(4)	18(3)	5(3)	0(3)
C(43')	39(4)	36(3)	69(4)	20(3)	8(3)	21(3)

C(44’)	49(4)	48(4)	50(4)	22(3)	-7(3)	15(3)
C(45’)	42(3)	31(3)	42(3)	14(3)	-1(3)	1(3)
C(46’)	26(3)	22(3)	33(3)	8(2)	4(2)	4(2)
C(51’)	35(3)	40(3)	41(3)	16(3)	5(3)	9(3)
C(52’)	57(4)	49(4)	52(4)	24(3)	16(3)	21(3)
C(53’)	75(5)	88(6)	46(4)	39(4)	27(4)	28(4)
C(54’)	100(6)	79(5)	37(4)	53(5)	15(4)	3(4)
C(55’)	70(4)	55(4)	38(4)	31(4)	11(3)	2(3)
C(56’)	32(3)	39(3)	30(3)	19(3)	3(2)	2(2)
O(1S)	146(7)	122(6)	128(6)	70(5)	9(5)	-41(5)
C(1S)	92(8)	100(8)	125(9)	15(6)	4(6)	26(7)
C(2S)	178(15)	176(14)	421(26)	129(14)	-108(16)	-151(15)
C(3S)	88(9)	199(19)	440(30)	51(12)	-27(13)	-101(19)
C(4S)	146(13)	91(9)	240(15)	-1(9)	-85(11)	-15(9)

[a]The anisotropic displacement factor exponent takes the form: $-2\pi^2(h^2a^{*2}U_{11} + ... + 2hka^*b^*U_{12})$

Table 3S. H-Atom Coordinates (x10^4) and Isotropic Displacement Coefficients (Å^{2}x10^3).

	x	y	z	U
H(8A)	3482	4983	1949	80
H(8B)	4481	4730	2261	80
H(8C)	4556	5143	1612	80
H(9A)	2002	2990	2214	80
H(9B)	2120	1906	2012	80
H(9C)	2974	2682	2515	80
H(10A)	1994	3843	1213	80
H(10B)	2835	3948	726	80
H(10C)	1931	2799	851	80
H(11A)	2896	689	-440	80
H(12A)	2106	1245	-1293	80
H(13A)	2558	3110	-1423	80
H(14A)	3716	4395	-692	80
H(15A)	4462	3843	164	80
H(21A)	1855	1286	761	80
H(22A)	-28	1	668	80
H(23A)	-417	-1856	635	80
H(24A)	1084	-2485	642	80
H(25A)	2962	-1175	779	80
H(31A)	3330	179	2094	80
H(32A)	3097	-1259	2735	80
H(33A)	4136	-2359	2643	80
H(34A)	5456	-1995	1940	80
H(35A)	5726	-536	1305	80
H(41A)	6791	1827	2157	80

H(42A)	8529	1707	2452	80
H(43A)	9727	1608	1740	80
H(44A)	9119	1497	720	80
H(45A)	7341	1507	435	80
H(51A)	5611	2342	-574	80
H(52A)	7061	3406	-1140	80
H(53A)	8692	4757	-683	80
H(54A)	8881	5064	349	80
H(55A)	7466	3963	930	80
H(8’A)	7309	3890	3359	80
H(8’B)	7266	4884	3006	80
H(8’C)	8287	5045	3477	80
H(9’A)	5156	3414	3662	80
H(9’B)	4769	4257	3978	80
H(9’C)	5050	4385	3311	80
H(10D)	6714	3461	4429	80
H(10E)	7694	4500	4731	80
H(10F)	6441	4226	4875	80
H(11B)	11027	8809	4015	80
H(12B)	12589	8328	3936	80
H(13B)	12488	6561	4144	80
H(14B)	10754	5274	4408	80
H(15B)	9200	5764	4512	80
H(21B)	10251	7832	5508	80
H(22B)	10515	7215	6448	80
H(23B)	8990	6044	6919	80
H(24B)	7148	5453	6431	80

H(25B)	6872	6073	5489	80
H(31B)	8230	8682	5935	80
H(32B)	7317	9263	6649	80
H(33B)	5601	9436	6384	80
H(34B)	4741	8924	5422	80
H(35B)	5630	8328	4702	80
H(41B)	8048	10490	4777	80
H(42B)	7569	11950	4459	80
H(43B)	6668	11857	3505	80
H(44B)	6216	10303	2883	80
H(45B)	6726	8660	3189	80
H(51B)	9632	10387	3652	80
H(52B)	10559	11143	2811	80
H(53B)	10601	9986	2018	80
H(54B)	9774	8102	2091	80
H(55B)	8867	7343	2941	80
H(1SA)	8078	4204	7327	80
H(1SB)	8001	3633	7928	80
H(2SA)	9548	3998	7250	80
H(2SB)	9014	2969	7622	80
H(3SA)	10189	3956	8277	80
H(3SB)	11015	4564	7802	80
H(4SA)	10294	5519	8528	80
H(4SB)	10648	5940	7903	80

For Table of Contents Use Only

Substitution Reactions of $(C_5Ph_5)Cr(CO)_3$: Structural, Electrochemical, and Spectroscopic Characterization of $(C_5Ph_5)Cr(CO)_2L$, L = PMe_3, PMe_2Ph, $P(OMe)_3$

D. John Hammack, Mills M. Dillard, Michael P. Castellani,* Arnold L. Rheingold,*
Anne L. Rieger, and Philip H. Rieger*

The series of compounds $(C_5Ph_5)Cr(CO)_2L$ (L = PMe_3, PMe_2Ph, $P(OMe)_3$) have been prepared and characterized by IR, NMR, and ESR spectroscopies, cyclic voltammetry, and X-ray crystallography (L = PMe_3). Frozen solution ESR studies and extended Hückel molecular orbital calcuations suggest the $Cr(CO)_2L$ moiety freely rotates relative to the C_5Ph_5 ligand.